



~~N62-72017~~
N63-12984
Code 1

TECHNICAL MEMORANDUM

X-193

INVESTIGATION OF THE LOW SUBSONIC FLIGHT CHARACTERISTICS
OF A MODEL OF A FLAT-TOP HYPERSONIC-BOOST GLIDE
CONFIGURATION HAVING AN ARROWHEAD WING

By Peter C. Boisseau

Langley Research Center
Langley Field, Va.

Declassified August 19, 1960

NATIONAL AERONAUTICS AND SPACE ADMINISTRATION
WASHINGTON

December 1959

NATIONAL AERONAUTICS AND SPACE ADMINISTRATION

TECHNICAL MEMORANDUM X-193

INVESTIGATION OF THE LOW SUBSONIC FLIGHT CHARACTERISTICS
OF A MODEL OF A FLAT-TOP HYPERSONIC-BOOST GLIDE
CONFIGURATION HAVING AN ARROWHEAD WING

By Peter C. Boisseau

SUMMARY

An investigation of the low subsonic flight characteristics of a model of a flat-top hypersonic-boost glide airplane has been made in the Langley full-scale tunnel over an angle-of-attack range from about 10° to 35° . Static force tests were made in the Langley free-flight tunnel.

The longitudinal stability and control characteristics were considered satisfactory when the model had positive static longitudinal stability. Flight could be maintained with neutral static longitudinal stability but the pilot had to pay close attention to pitch control. The model had a mild pitchup tendency at the higher angles of attack (25° to 35°). The lateral stability and control characteristics were considered to be fair at the lower angles of attack (10° to 15°). As the angle of attack increased, the Dutch roll oscillation became less damped until at an angle of attack of 20° the model had a constant-amplitude oscillation. The model became unstable at the higher angles of attack and went out of control at an angle of attack of about 25° . Artificial damping in roll greatly improved the Dutch roll damping and made it possible for the model to be flown to an angle of attack of 35° .

INTRODUCTION

An investigation is being conducted by the National Aeronautics and Space Administration to provide information on the stability and control characteristics of some proposed hypersonic-boost glide configurations over the speed range from hypersonic to low subsonic speeds. (For example, see refs. 1 to 4.) The present investigation was made to provide some information at low subsonic speeds on the longitudinal and lateral stability and control characteristics of a model of a flat-top

hypersonic-boost glide configuration having an arrowhead wing with a leading-edge sweep of 77.4° and with the wing tips drooped 45° .

The investigation included flight tests in the Langley full-scale tunnel to determine the low-speed flight characteristics of the model over an angle-of-attack range from about 10° to 35° and force tests in the Langley free-flight tunnel to determine the static stability and control characteristics over an angle-of-attack range from 0° to 40° .

Included in the flight-test investigation was a study to determine the effect of center-of-gravity location on the longitudinal stability and control characteristics. These tests were made at an angle of attack of 17° . Also studied in the flight tests was the effect of artificial roll damping on the lateral stability and control characteristics.

L.
6
5
8

SYMBOLS

The lateral data are referred to the body system of axes (see fig. 1) and the longitudinal data are referred to the wind system of axes. All moments are measured about a center-of-gravity position located longitudinally at 29.5 percent of the mean aerodynamic chord and vertically at 4.4 percent of the mean aerodynamic chord below the top surface of the wing at the plane of symmetry. All measurements are reduced to standard coefficient form and are based on the wing without tip droop.

| | |
|------------|--|
| X,Y,Z | coordinate axes |
| S | wing area, sq ft |
| \bar{c} | wing mean aerodynamic chord, ft |
| V | airspeed, ft/sec |
| b | wing span, ft |
| ρ | air density, slug/cu ft |
| p | rolling velocity, radians/sec |
| q | dynamic pressure, $\frac{\rho V^2}{2}$, lb/sq ft |
| α | angle of attack, deg |
| δ_e | elevator deflection (elevons deflected together for elevator control), deg |

| | |
|--------------------------------------|--|
| δ_a | aileron deflection (elevons deflected differentially for aileron control), deg |
| δ_r | rudder deflection, deg |
| β | angle of sideslip, deg |
| I_X, I_Y, I_Z | moments of inertia |
| F_D | drag force, lb |
| F_Y | side force, lb |
| F_L | lift force, lb |
| M_Y | pitching moment, ft-lb |
| M_X | rolling moment, ft-lb |
| M_Z | yawing moment, ft-lb |
| C_D | drag coefficient, $\frac{F_D}{qS}$ |
| C_Y | lateral-force coefficient, $\frac{F_Y}{qS}$ |
| C_L | lift coefficient, $\frac{F_L}{qS}$ |
| C_m | pitching-moment coefficient, $\frac{M_Y}{qS\bar{c}}$ |
| C_n | yawing-moment coefficient, $\frac{M_Z}{qSb}$ |
| C_l | rolling-moment coefficient, $\frac{M_X}{qSb}$ |
| $\Delta C_Y, \Delta C_n, \Delta C_l$ | incremental force and moments |
| $C_{Y\beta}$ | side-force parameter, $\left(\frac{\Delta C_Y}{\Delta \beta} \right)_{\beta=\pm 5^\circ}$ |

$C_{n\beta}$ directional-stability parameter, $\left(\frac{\Delta C_n}{\Delta \beta}\right)_{\beta=\pm 5^\circ}$

$C_{l\beta}$ effective-dihedral parameter, $\left(\frac{\Delta C_l}{\Delta \beta}\right)_{\beta=\pm 5^\circ}$

$$C_{np} = \frac{\partial C_n}{\partial \left(\frac{pb}{2V}\right)}$$

APPARATUS AND TESTING TECHNIQUE

Model

The same model was used for both the static and dynamic portions of the investigation. A three-view drawing of the model is shown in figure 2, and a photograph of the model is shown in figure 3. Table I gives the dimensional and mass characteristics of the model. The trailing edges of the drooped wing tips act as elevons and provide roll control as well as longitudinal control.

For the flight tests, thrust was provided by compressed air supplied through flexible hoses to two nozzles at the rear of the fuselage. The amount of thrust could be varied and the maximum output per nozzle was about 10 to 12 pounds. The controls were operated remotely by the pilots by means of flicker-type (full on or off) pneumatic servomechanisms which were actuated by electric solenoids. Artificial stabilization in roll was provided by a simple rate damper. An air-driven rate gyro was the sensing element and the signal was fed into a servo-actuator which deflected the elevons in proportion to the rolling velocity. The manual control was superimposed on the control deflection resulting from the rate signal.

Test Equipment and Setup

The force tests were conducted in the Langley free-flight tunnel. The model was mounted on a small-diameter sting. (Sting cross-sectional area was 2.3 percent of the fuselage base area.) The forces and moments were measured about the body axes by means of three-component strain-gage balances.

The flight investigation was conducted in the Langley full-scale tunnel with the test setup illustrated in figure 4. A complete description

of the test technique used in making the free-flying model tests is given in reference 5.

STATIC STABILITY AND CONTROL CHARACTERISTICS OF FLIGHT-TEST MODEL

L Force tests were made in the Langley free-flight tunnel to deter-
6 mine the static longitudinal and lateral stability and control charac-
5 teristics of the model over an angle-of-attack range from 0° to 40° .
8 These tests were run at a dynamic pressure of 4.4 pounds per square foot,
which corresponds to an airspeed of about 61 feet per second at standard
sea-level conditions and to a test Reynolds number of 1.43×10^6 based on
the mean aerodynamic chord of 3.67 feet.

Static Longitudinal Stability and Control

The static longitudinal stability characteristics of the model are presented in figure 5 for elevator deflections of 0° , -10° , and -20° . These data show that the model was longitudinally stable up to an angle of attack of about 24° and then became unstable. The slope of the pitching-moment curve for $\delta_e = 0^\circ$ at $C_L = 0$ indicates that the aerodynamic-center location is at 41 percent of the mean aerodynamic chord.

The data of reference 3 indicate that the aerodynamic center of a generally similar configuration is at 0.558 but this apparent discrepancy can be explained by the difference in the method used in calculating the location of the mean aerodynamic chord in the two cases. The mean-aerodynamic-chord location used in reference 3 was determined by fitting the mean aerodynamic chord to the wing so that it extended from the leading edge to the trailing edge of the defined area. Since this wing had a discontinuity in plan form, the location of the mean aerodynamic chord in the present report was determined by the conventional method presented in aeronautical textbooks for determining the mean aerodynamic chord of wings having two or more wing panels of different shapes. These data also show that elevator deflection produced a nearly constant increment of pitching moment over the angle-of-attack range and that the elevator deflection had only a small effect on the lift coefficient.

Static Lateral Stability and Control

Force tests were made to determine the static lateral stability and control characteristics of the model with and without the ventral tail over a sideslip range of $\pm 20^\circ$ and for angles of attack from 0° to 40° .

The lateral stability characteristics are presented in figure 6. The data of figure 6 are summarized in figure 7 as the variation with angle of attack of the side-force parameter $C_{Y\beta}$, the directional-stability parameter $C_{N\beta}$, and the effective-dihedral parameter $C_{l\beta}$, which were obtained by measuring the slopes of the curves at angles of sideslip between -5° and 5° . The data of figure 7 show that there was a gradual decrease in directional stability as the angle of attack increased until the model became directionally unstable above angles of attack of 27° or 28° . The data also show that the ventral tail produced a nearly constant increment of directional stability over the entire angle-of-attack range. Because of the negative geometric dihedral of the wing tips, the model had negative effective dihedral up to an angle of attack of about 5° . Positive effective dihedral $-C_{l\beta}$ occurred over the remainder of the angle-of-attack range.

L
6
5
8

The variation of the aileron control effectiveness with angle of attack is presented in figure 8. These data show that the rolling and yawing moments produced by the ailerons were fairly constant up to an angle of attack of 32° and then decreased. It should be noted that the ailerons produced over twice as much favorable yawing moment as rolling moment over the angle-of-attack range. This effect is due to the fact that the ailerons are on the drooped wing tips. The data of figure 9 show that the yawing moment produced by rudder deflection remains about constant up to an angle of attack of about 12° before it drops off slightly.

FLIGHT TESTS

Flight tests were made to study the dynamic stability and control characteristics of the model over an angle-of-attack range from about 10° to 35° . Flights were made at an angle of attack of 17° to determine the effect of center-of-gravity position on the longitudinal characteristics of the model. Flights were also made over the angle-of-attack range to determine the effect of artificial roll damping on the lateral stability and control characteristics.

Flights were made with coordinated aileron and rudder control and also with ailerons alone. The flicker type (full on or off) control deflections used for most of the flight tests were $\delta_a = \pm 8^\circ$, $\delta_r = \pm 20^\circ$, and $\delta_e = \pm 10^\circ$. These deflections were from the trimmed position of the control surfaces for a particular flight condition.

The model behavior during flight was observed by the pitch pilot located at the side of the test section and by the roll and yaw pilot

located in the rear of the test section. The results obtained in the flight tests were primarily in the form of qualitative ratings of flight behavior based on pilot opinion. Motion-picture records obtained in the tests were used to verify and correlate the ratings for the different flight conditions.

FLIGHT-TEST RESULTS AND DISCUSSION

A motion-picture film supplement covering flight tests of the model has been prepared and is available on loan. A request card form and a description of the film will be found at the back of this paper, on the page immediately preceding the abstract and index pages.

Longitudinal Stability and Control

During the investigation made to study the longitudinal stability and control characteristics of the model, artificial damping in roll was used in order to minimize any effects lateral motions might exert on the longitudinal behavior.

As part of the longitudinal investigation a series of flights were made at an angle of attack of 17° to determine the effect of center-of-gravity location. Static tests indicated that at this angle of attack the model was neutrally stable at a center-of-gravity position of about 36 percent of the mean aerodynamic chord. With the center of gravity forward of this point the model flew smoothly and the pilot had no trouble in controlling it. With neutral stability the model reacted rather sharply to gusts and control disturbances and the pilot had to pay very close attention to the elevator control at all times to keep the model flying. This was the most rearward center-of-gravity position at which sustained flights could be made. When the center of gravity was moved slightly rearward of the 36-percent-chord position, the model could be flown as long as it was not violently disturbed; but once the model was sufficiently disturbed, it diverged in pitch despite the use of corrective control. The results of the model flight tests of reference 5 indicated that the model could have been flown with small amounts of static instability if the longitudinal control power could have been increased. It did not seem feasible, however, to increase the longitudinal control deflection beyond the value of $\pm 10^\circ$ used in these tests. Results of the tests of reference 5 and of the analog studies of reference 6 showed that the use of artificial damping in pitch would afford a definite improvement in the longitudinal characteristics for statically unstable conditions.

In addition to the center-of-gravity range studies made at an angle of attack of 17° , flights were made at angles of attack from 10° to 35° with a center-of-gravity position (29.5 percent \bar{c}) that gave good static longitudinal stability at an angle of attack of 17° . The longitudinal characteristics of the model were generally satisfactory at angles of attack up to about 25° or 30° where the model had a pitchup tendency. (See fig. 5.) It was possible to fly the model up to maximum lift ($\alpha = 35^\circ$) by careful use of the pitch control, however, because the static stability was about neutral at angles of attack beyond the pitchup.

Lateral Stability and Control

No roll damping added.- The lateral stability and control characteristics of the model were considered to be only fair at the lower angles of attack (10° to 15°). The Dutch roll oscillation was lightly damped and close attention to control was required to keep the model flying because of low control effectiveness. It was difficult to fly the model smoothly not only because of the low damping of the Dutch roll oscillation but also because of the large favorable yawing moments produced by the elevons. (See fig. 8.) It was sometimes very difficult to recover the model from large disturbances because of the low control effectiveness.

As the angle of attack increased, the oscillation became less damped and at an angle of attack of about 20° the model had a constant-amplitude Dutch roll oscillation. Although the yawing motions associated with the Dutch roll oscillation increased as the angle of attack increased (probably because of the decrease in directional stability) the character of the oscillation was still primarily a rolling motion because of the large ratios of I_Z/I_X and C_{l_β}/C_{n_β} . As the angle of attack increased further, the oscillation became unstable and the model went out of control at about an angle of attack of 25° despite efforts by the pilot to control it.

The control characteristics of the model became progressively worse as the angle of attack increased, probably because the large favorable yawing moments produced by the roll control created larger yawing motions of the model as the directional stability decreased.

The flat-bottom boost-glide model of reference 4 had about the same dynamic lateral stability characteristics as the flat-top model of the present investigation but it had much better overall lateral flight behavior apparently because it had better lateral control characteristics.

Roll damping added.- The addition of artificial roll damping to improve the stability of the Dutch roll oscillation greatly improved the lateral control characteristics of the model so that flights could be made up to maximum lift ($\alpha = 35^\circ$) where the model diverged in sideslip. Although the rate damper increased the damping in roll, it also introduced large negative values of C_{n_p} (because of the yawing moments produced by the elevons) which probably made the behavior of the model somewhat more erratic than it would have been if only damping in roll had been added.

During flights with rudder fixed and ailerons alone used for control, the behavior of the model was generally similar to that of the model with coordinated ailerons and rudder except that without the rudder control it was more difficult to recover from a disturbance. This was particularly true whenever there was any sidewise motion of the model. In flights made with the ventral tail removed, the lateral stability characteristics were still generally similar to those for the case with the rudder fixed and ailerons alone used for control.

CONCLUSIONS

The results of the investigation are as follows:

1. The longitudinal stability and control characteristics of the model were considered satisfactory when the model had positive static longitudinal stability. Flights could be maintained with neutral stability but the pilot had to pay close attention to elevator control. The model had a mild pitchup tendency at the higher angles of attack (25° to 30°).

2. The lateral stability and control characteristics were considered to be fair at the lower angles of attack flown (10° to 15°). As the angle of attack increased, the Dutch roll oscillation became less damped until at an angle of attack of 20° the model had a constant-amplitude oscillation. The model became unstable at higher angles of attack and went out of control at an angle of attack of about 25° . The control characteristics of the model became progressively worse as the angle of attack increased. Artificial damping in roll greatly improved the Dutch roll damping and made it possible for the model to be flown to an angle of attack of 35° .

Langley Research Center,
National Aeronautics and Space Administration,
Langley Field, Va., August 27, 1959.

REFERENCES

1. Syvertson, Clarence A., Gloria, Hermilo R., and Sarabia, Michael F.: Aerodynamic Performance and Static Stability and Control of Flat-Top Hypersonic Gliders at Mach Numbers From 0.6 to 18. NACA RM A58G17, 1958.
2. Kelly, Mark W.: Wind-Tunnel Investigation of the Low-Speed Aerodynamic Characteristics of a Hypersonic Glider Configuration. NACA RM A58F03, 1958.
3. Buell, Donald A., and Johnson, Norman S.: Stability and Control Characteristics at Subsonic Speeds of a Flat-Top Arrowhead Wing-Body Combination. NASA MEMO 3-5-59A, 1959.
4. Rainey, Robert W.: Static Stability and Control of Hypersonic Gliders. NACA RM L58E12a, 1958.
5. Paulson, John W., and Shanks, Robert E.: Investigation of Low-Subsonic Flight Characteristics of a Model of a Flat-Bottom Hypersonic-Boost Glide Configuration Having a 78° Delta Wing. NASA TM X-201, 1959.
6. Moul, Martin T., and Brown, Lawrence W.: Effect of Artificial Pitch Damping on the Longitudinal and Rolling Stability of Aircraft With Negative Static Margins. NASA MEMO 5-5-59L, 1959.

L
6
5
8

TABLE I.- DIMENSIONAL AND MASS CHARACTERISTICS
OF THE TEST MODEL

| | |
|---|--------------|
| Weight, lb | 35.8 |
| Moments of inertia: | |
| I_X , slug-ft ² | 0.32 |
| I_Y , slug-ft ² | 4.25 |
| I_Z , slug-ft ² | 4.69 |
| Wing: | |
| Airfoil section | Single wedge |
| Area (without wing-tip droop), sq ft | 10.75 |
| Span (without wing-tip droop), ft | 3.67 |
| Span (with wing-tip droop), ft | 3.25 |
| Aspect ratio | 0.98 |
| Root chord, ft | 5.97 |
| Tip chord, ft | 0 |
| Mean aerodynamic chord (without wing-tip droop), ft | 3.67 |
| Sweep of leading edge, deg | 77.4 |
| Sweep of trailing edge, deg | 17.6 |
| Wing-tip droop, deg | 45 |
| Leading-edge diameter, ft | 0.003 |
| Elevons (each): | |
| Airfoil section | Flat plate |
| Span, ft | 0.69 |
| Area, sq ft | 0.73 |
| Aspect ratio | 0.65 |
| Root chord, ft | 0.57 |
| Tip chord, ft | 0.50 |
| Ventral tail: | |
| Airfoil section | Double wedge |
| Span, ft | 0.40 |
| Total area, sq ft | 0.36 |
| Rudder area, sq ft | 0.24 |
| Aspect ratio | 0.46 |
| Root chord, ft | 1.30 |
| Tip chord, ft | 0.32 |

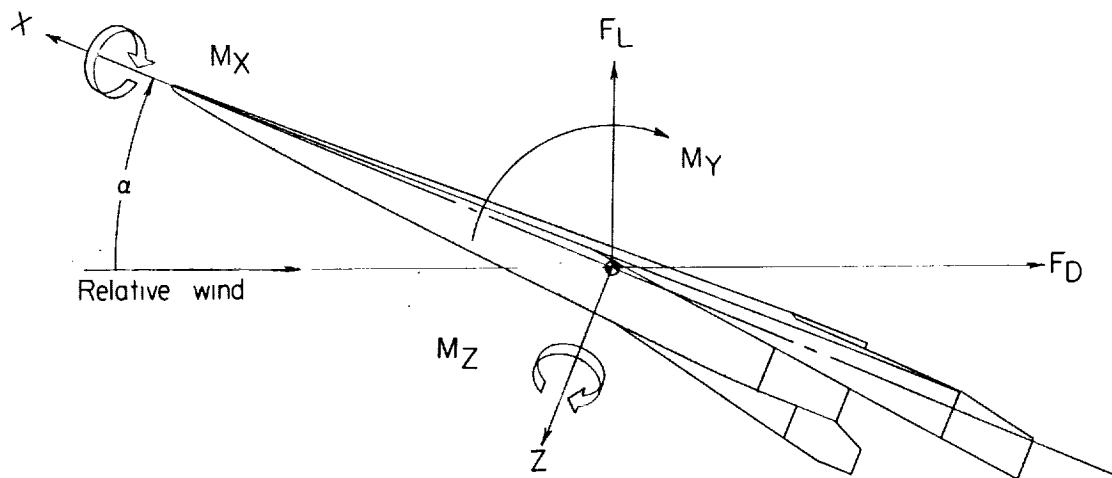
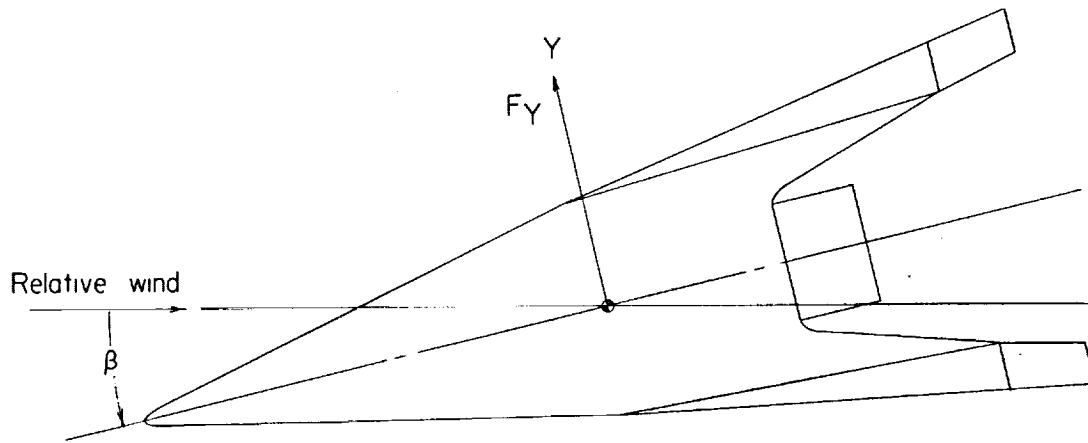


Figure 1.- System of axis used in investigation. Longitudinal data are referred to wind system of axes, and lateral data are referred to body system of axes. Arrows indicate positive directions of moments, forces, and angles.

L-658

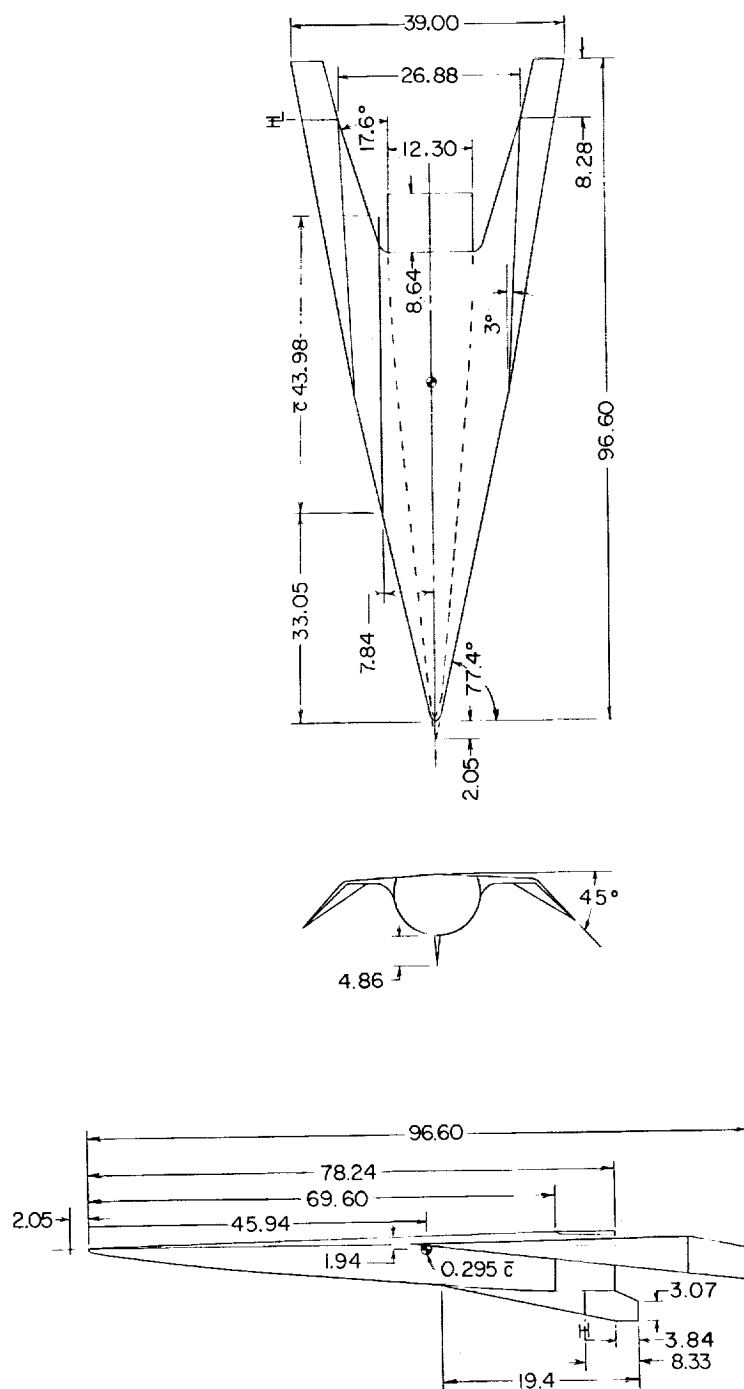


Figure 2.- Three-view drawing of 1/10-scale model of the flat-top hypersonic-boost glide airplane used in the investigation. All dimensions are in inches.

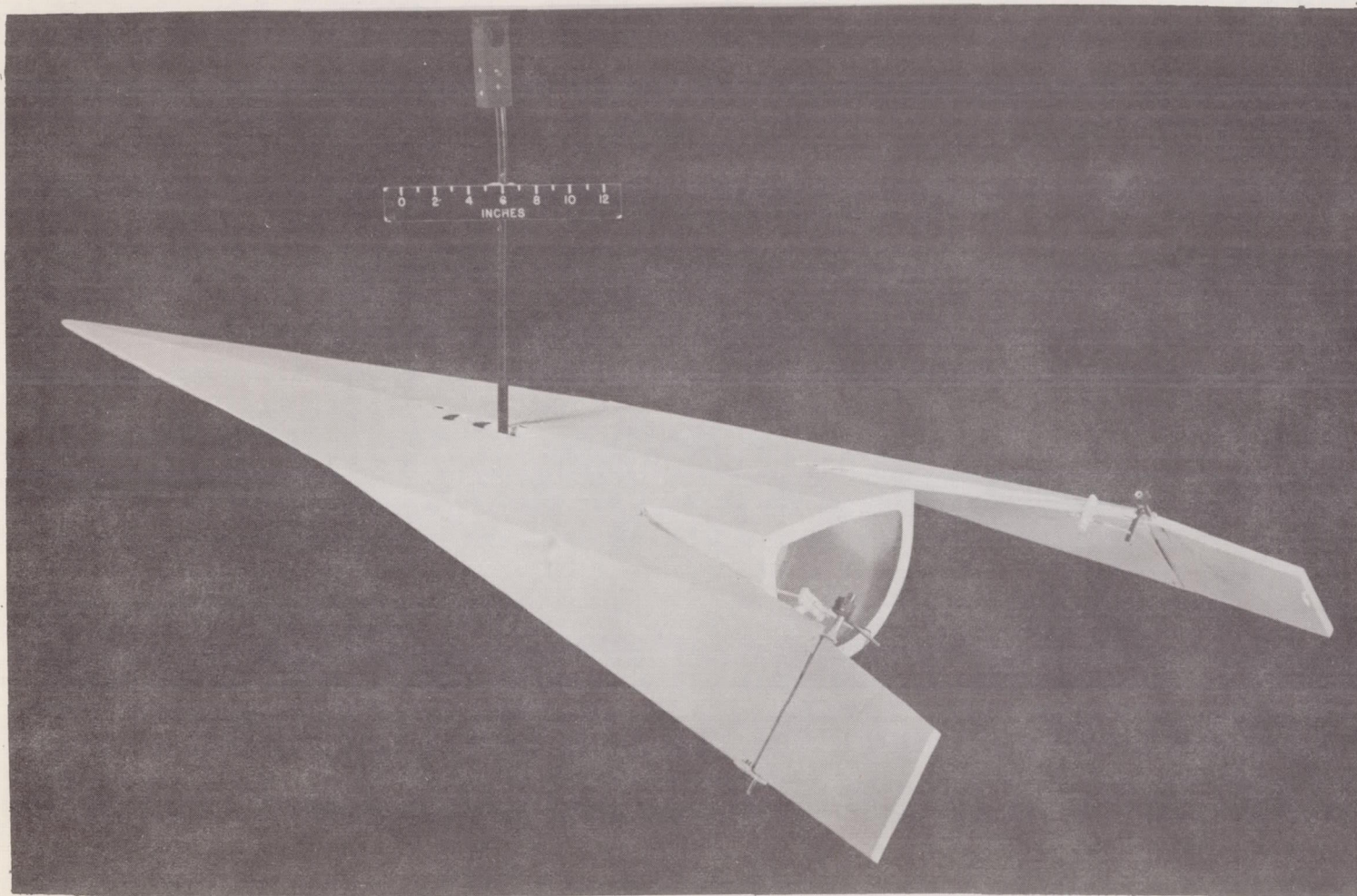


Figure 3.- Photograph of model used in investigation. L-57-4842

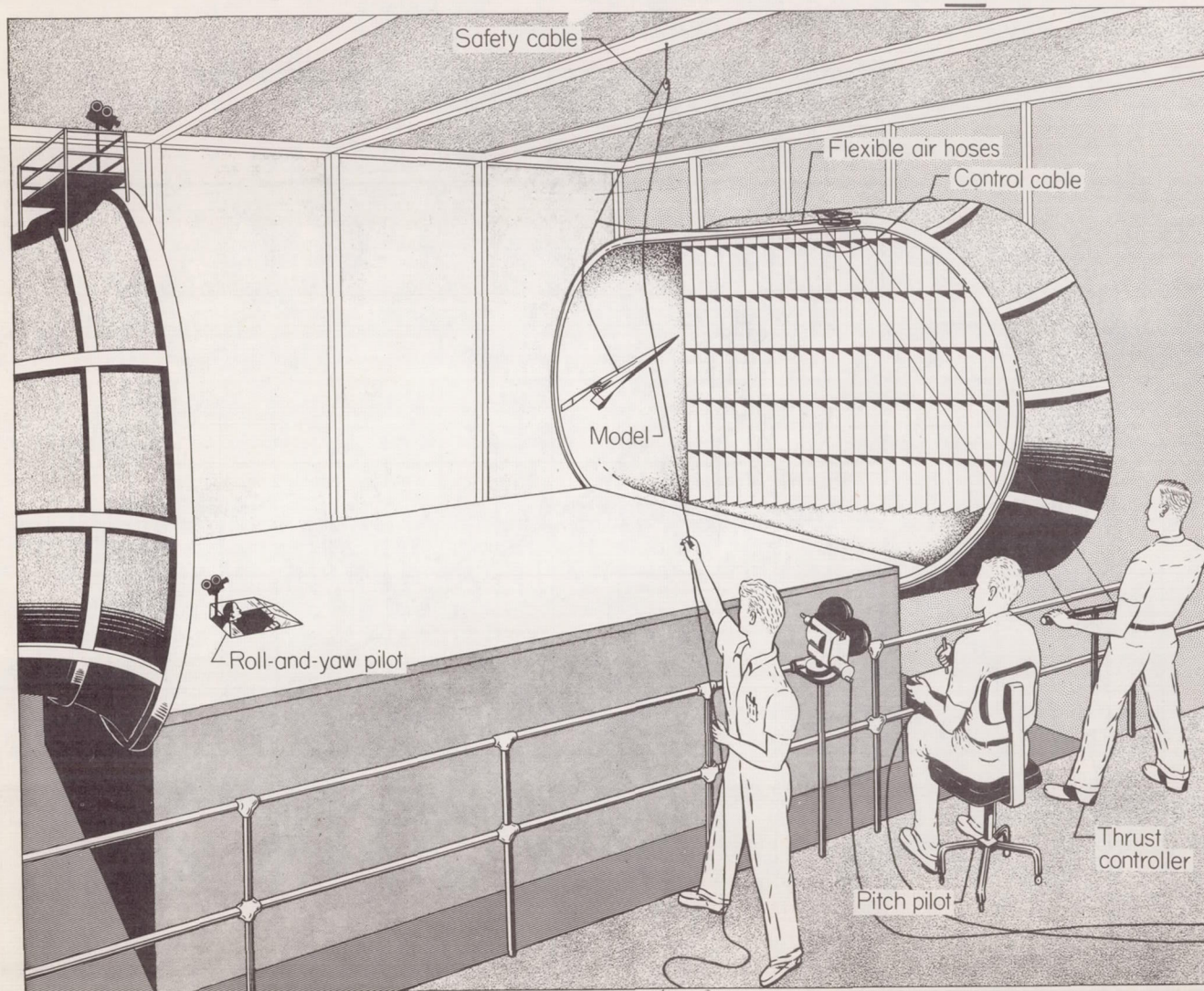


Figure 4.- Sketch of test setup in Langley full-scale tunnel.

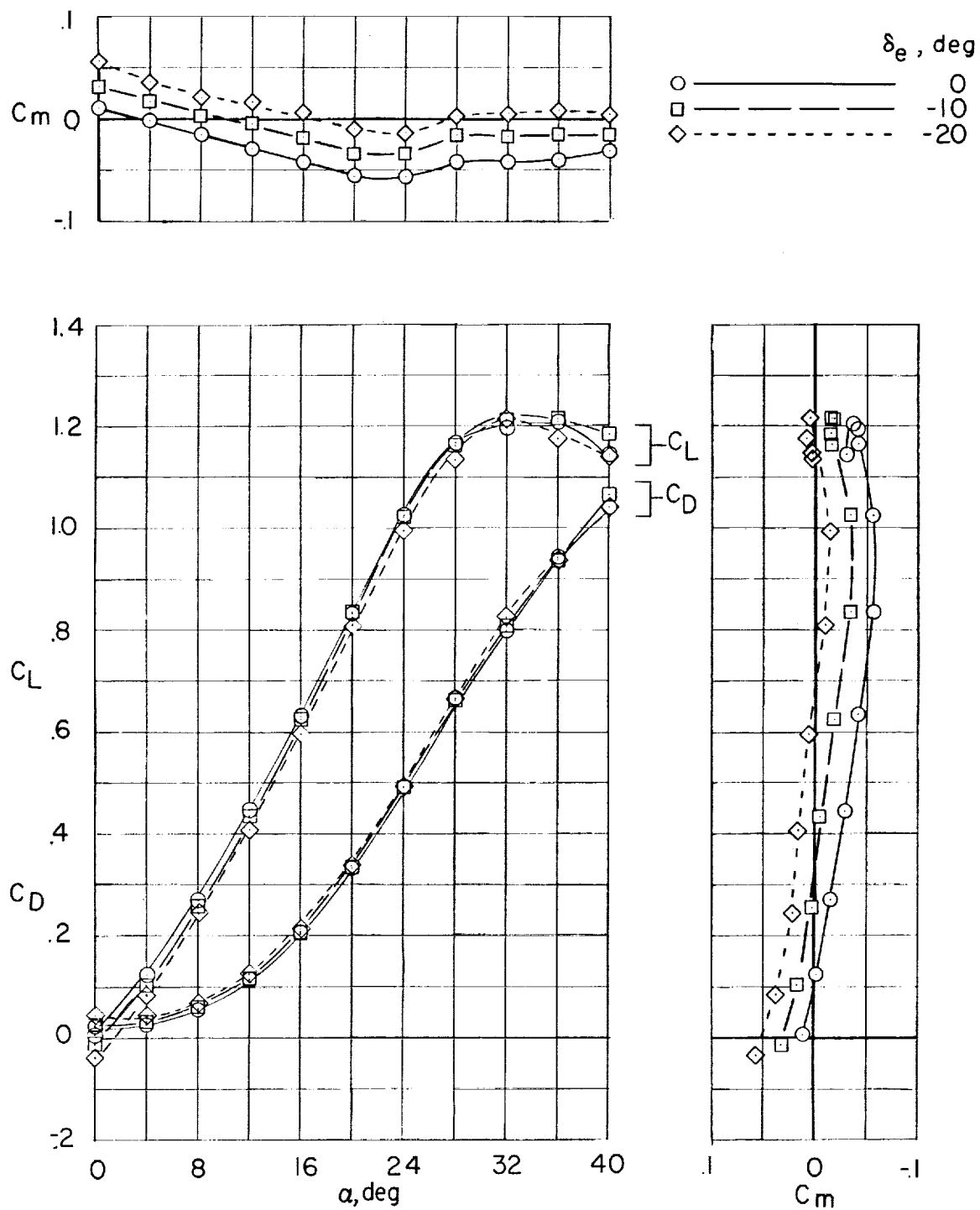
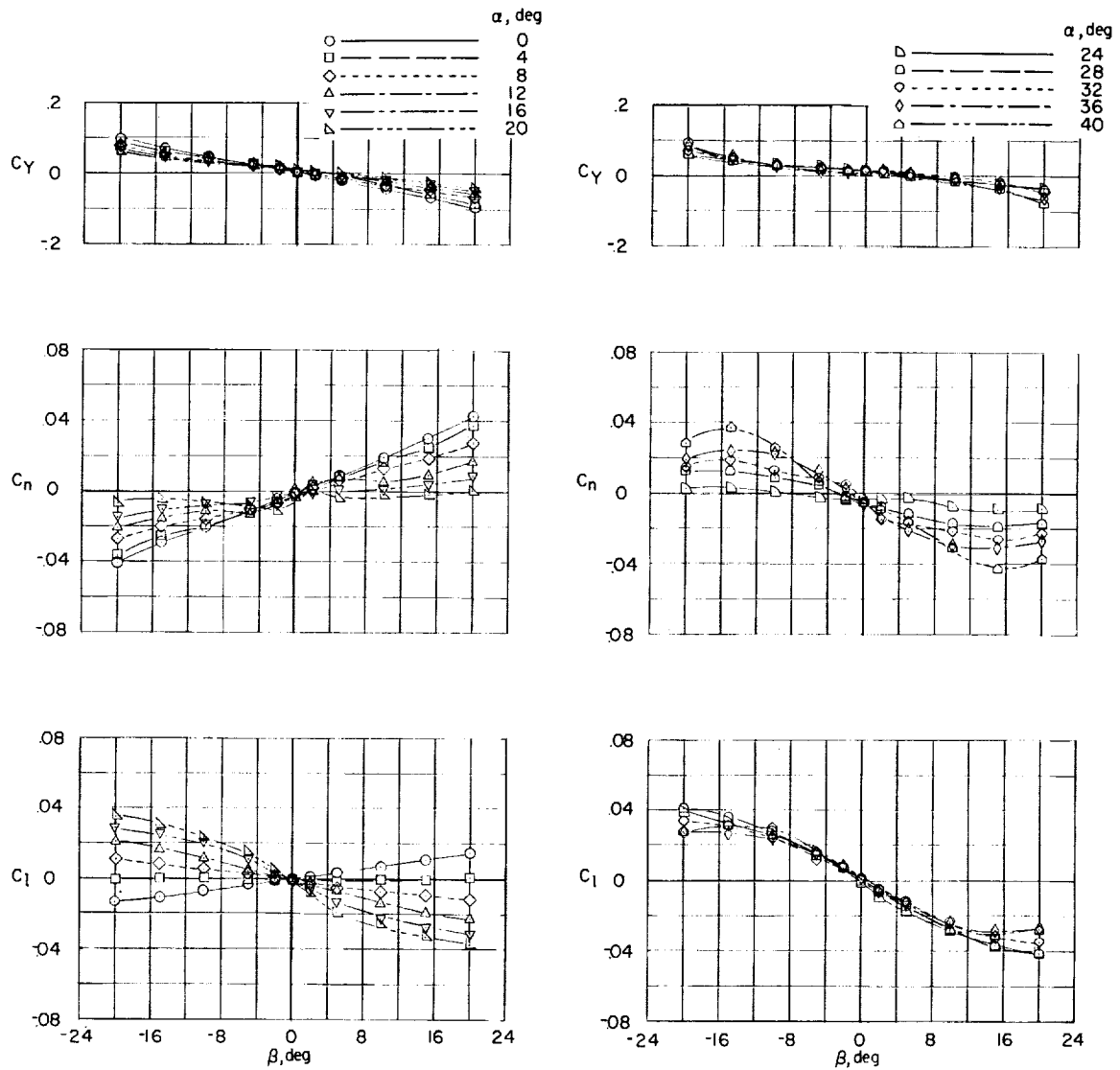


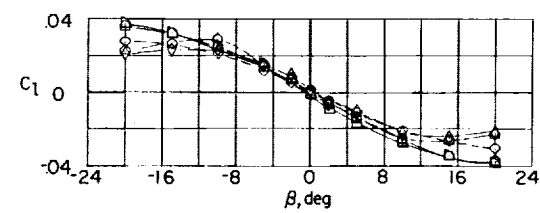
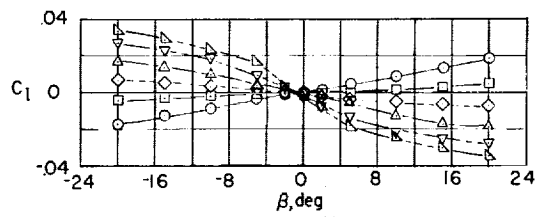
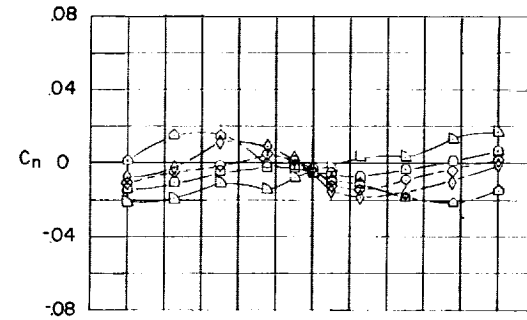
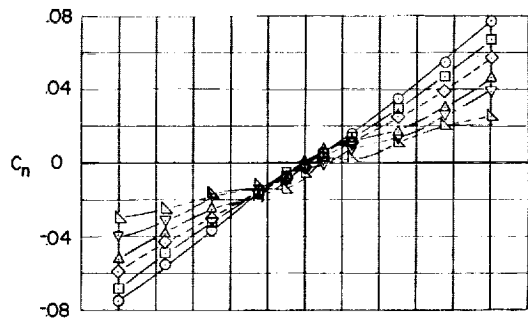
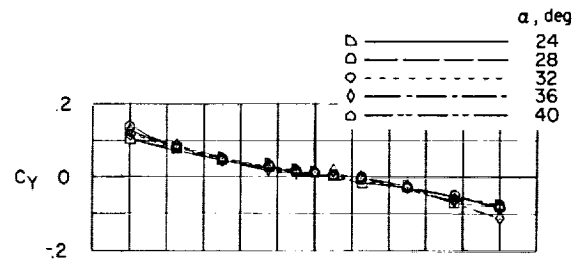
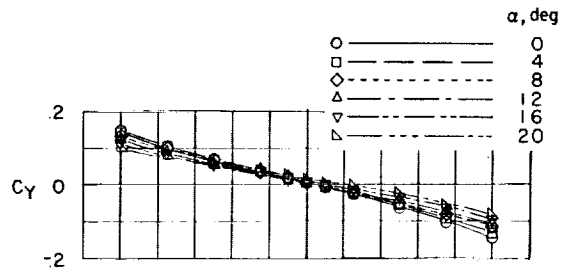
Figure 5.- Longitudinal characteristics of model.

L-658



(a) Ventral tail off.

Figure 6.- Variation of static lateral stability characteristics with angle of sideslip. $\delta_e = -10^\circ$.



(b) Ventral tail on.

Figure 6.- Concluded.

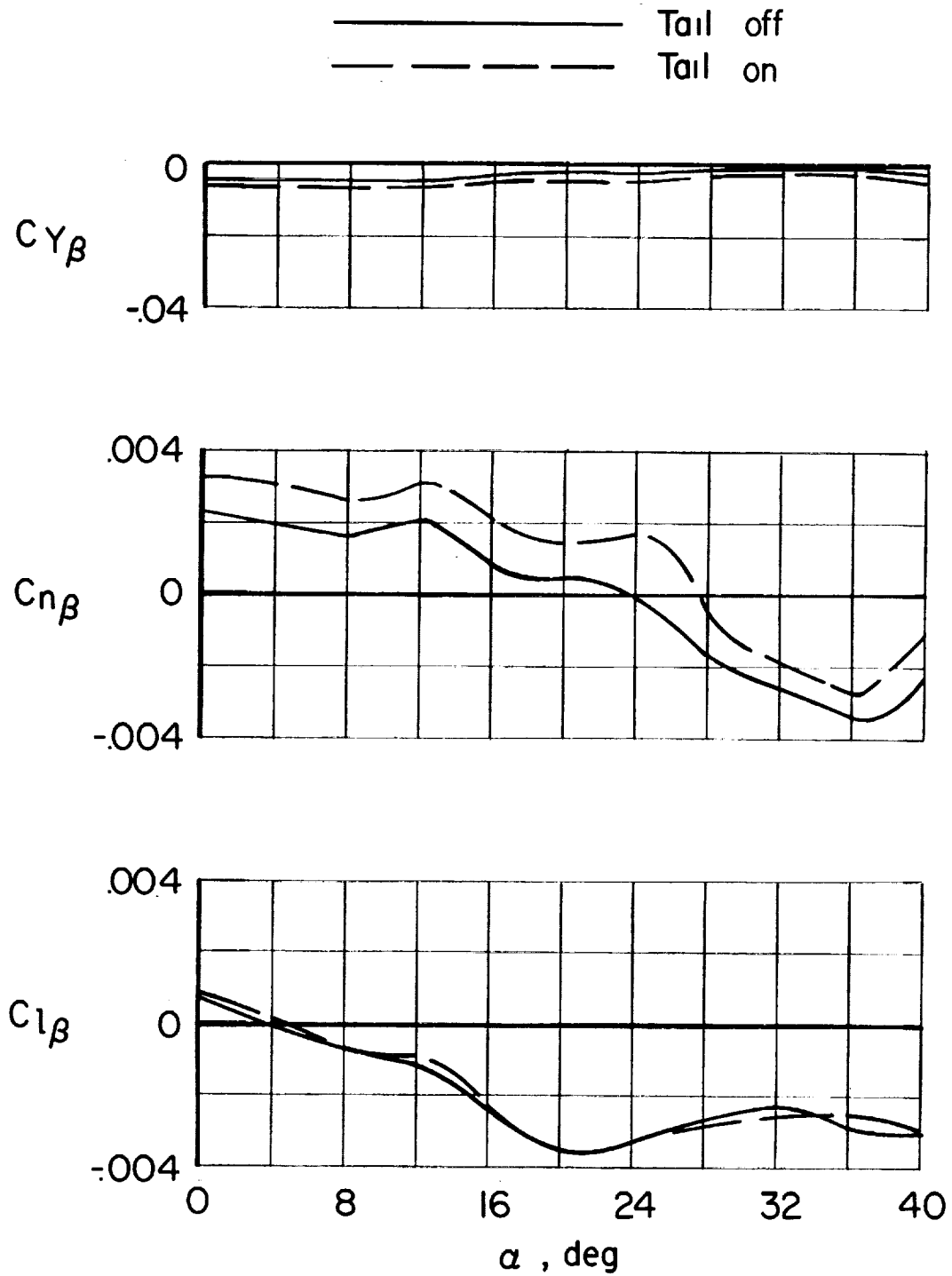


Figure 7.- Variation of static sideslip derivatives with angle of attack.
 $\beta = \pm 5^\circ$; $\delta_e = -10^\circ$.

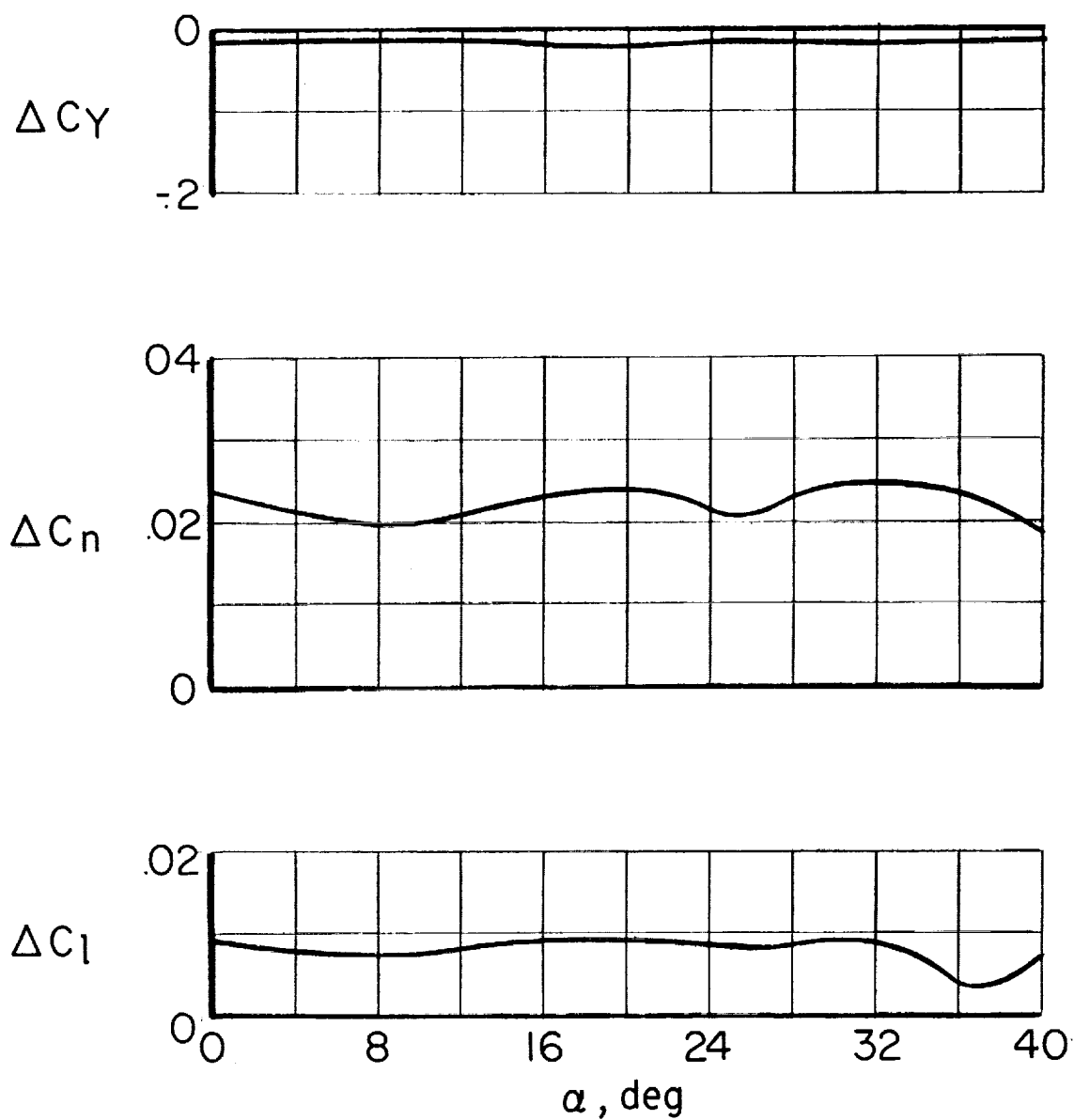


Figure 8.- Increments of lateral-force and moment coefficients produced by differential deflection of the elevons of $\pm 20^\circ$.

L-658

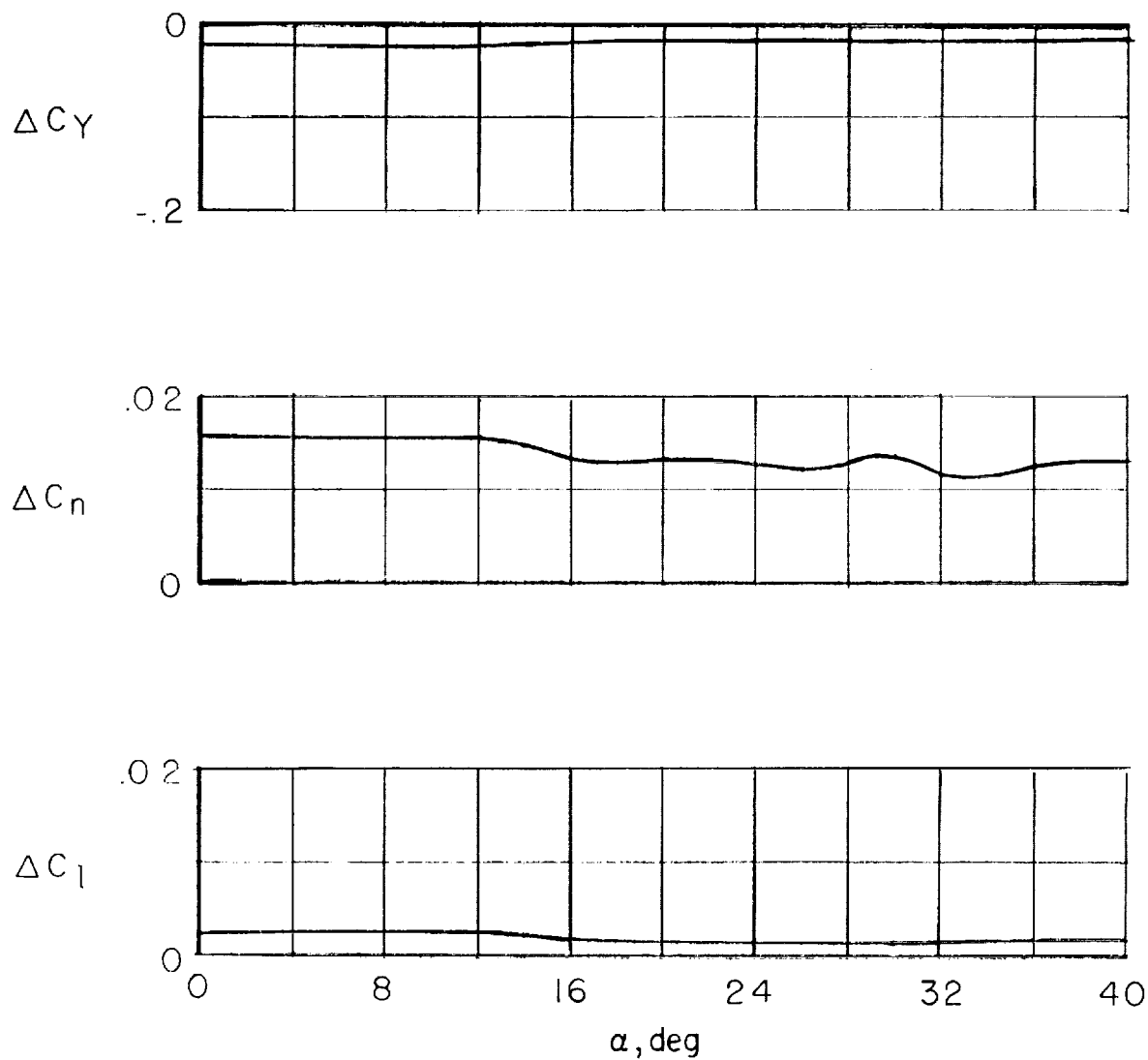


Figure 9.- Increments of lateral-force and moment coefficients produced by deflection of the rudder of -20° .